Dynamic Imaging Motion Artifact Reduction using Adaptive K-Space Polynomial Interpolation

T. B. Smith[1], and K. S. Nayak[1]
[1]Electrical Engineering, University of Southern California, Los Angeles, CA, United States

Introduction: Dynamic imaging is vulnerable to data inconsistency artifacts caused by object movement between acquisitions. These artifacts occur because the k-t energy M(**k**,t) of the dynamic object is incompletely sampled. In sliding window reconstructions (SW), the manifestation of these artifacts depends on the k-space sampling trajectory; for example, they appear as ghosts in echo-planar imaging and swirling noise in spiral imaging [1]. Reconstruction using linear interpolation (LI) or low-pass filtering (LPF) along the temporal dimension can help mitigate these artifacts [2]. With LPF, filters with lower cutoff frequencies do better at reducing artifacts but also induce more motion blur. In this work, we present an adaptive polynomial interpolation (API) algorithm which automatically determines the appropriate cutoff frequency for each **k** location and each image frame time t using the local variation of M(**k**,t).

Methods: We define **s** to be the array of T samples of M(**k**,t) acquired in some local (temporal) neighborhood around the image frame time. We assume the values in **s** are samples from a polynomial with unknown degree W. The measured data is $\mathbf{y} = \mathbf{s} + \mathbf{n}$, where **n** is AWGN with covariance $\sigma^2\mathbf{I}$. API jointly estimates the degree and the coefficients of the polynomial from **y**, and then evaluates the estimated polynomial at the frame time to construct the interpolated value. The estimated degree $\hat{W}$ must lie in the interval [0,T–1]. When $W \geq T-1$ or when **s** is not modeled well by a polynomial, $\hat{W} = T-1$ and API uses linear interpolation.

To estimate the degree of the underlying polynomial, **y** is projected onto a sequence of polynomial subspaces with increasing dimension until the residual energy is dominated by noise. If we define P_N to be the projection matrix for an N^{th}-degree polynomial basis (eg, $P_N = V_N(V_N^T V_N)^{-1}V_N^T$ where V_N is the N^{th} order Vandermonde matrix), then the least-squares estimate of **s** is $\hat{\mathbf{s}}_N = P_N\mathbf{y}$ and the residual is $\boldsymbol{\varepsilon}_N = \mathbf{y} - \hat{\mathbf{s}}_N$. It can be shown that $E[\|\boldsymbol{\varepsilon}_N\|^2] = \mathbf{s}^H[P_N - I]\mathbf{s} + (T-N)\sigma^2$. When N is large enough so that the range of P_N contains **s** (ie, $N \geq W$), then $\mathbf{s}^H[P_N - I]\mathbf{s} = 0$. To estimate $\hat{W}$, we therefore find the smallest N for which $\|\boldsymbol{\varepsilon}_N\|^2 < (T-N)\sigma^2$ and set $\hat{W} = N$.

After estimating $\hat{W}$, API forms the weight vector $\mathbf{h} = \mathbf{t}^T(V_{\hat{W}}^T V_{\hat{W}})^{-1}V_{\hat{W}}^T$, where **t** is the Vandermonde vector for the image frame time. The interpolation weights **h** can be viewed as a FIR filter that varies with k-t location, and whose output $\mathbf{h}^T\mathbf{y}$ is the interpolated value. Fig. 1 shows example frequency responses of **h** for various values of $\hat{W}$. When the data are locally smooth, API uses a more aggressive low-pass filter to improve artifact reduction. Otherwise, API uses less filtering to avoid motion blur while still providing some artifact reduction.

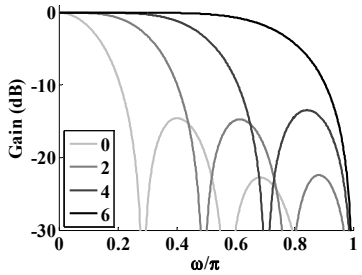

Fig. 1: Frequency responses of the low-pass filters in API (T = 8) for various $\hat{W}$.

Results and Discussion: Fig. 2 shows example frames in a 17-frame sequence from a dynamic spiral imaging study of the upper airway. Frames 3, 7, and 12 exhibit increasing levels of artifacts due to data inconsistencies. Compared to SW, LPF reconstruction has little artifact energy but heavy motion blurring of the tongue and velum. The LI frames have almost no blurring, but little artifact reduction. API exhibits little blurring and good artifact reduction.

To quantify these results, three regions of interest (ROI)—the tongue, velum, and airway—were manually segmented using the API images for each frame. The ratios of average pixel energy in the ROIs are shown in Fig. 3 for each reconstruction method. Smaller airway energy indicates more artifact reduction and less blur, while larger tongue and velum energy indicates better signal level. As seen in Fig. 3, API produces the best energy ratio in nearly every frame.

The API algorithm is flexible and can accommodate temporally non-uniformly sampled data and aperiodic object motion. It does not require training, only an estimate of each coil's noise variance and a neighborhood T. Also, it may be amenable to real time systems if more efficient (eg, Newton, Lagrange) polynomial formats are used.

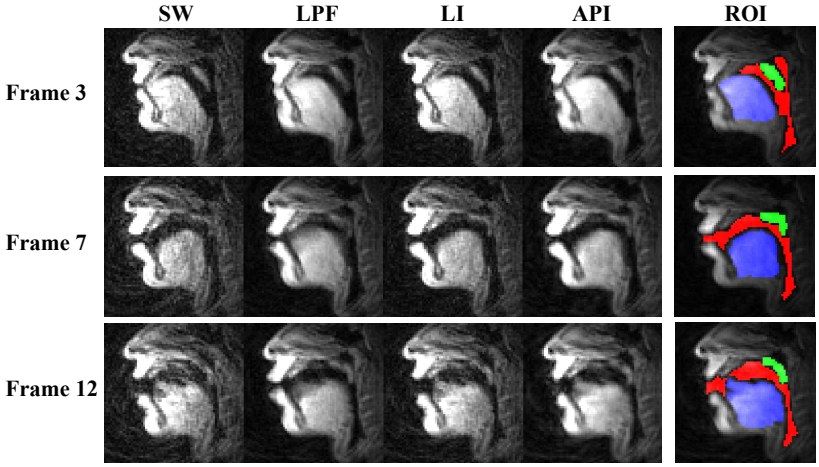

Fig. 2: Reconstructions of the upper airway anatomy from 13-interleaf spiral data (TR = 6.5 ms, frame interval = 45.5 ms). The LPF cutoff frequency was π/13, and API used T = 7. ROI shows the airway (red), tongue (blue), and velum (green) pixels used in Fig. 3.

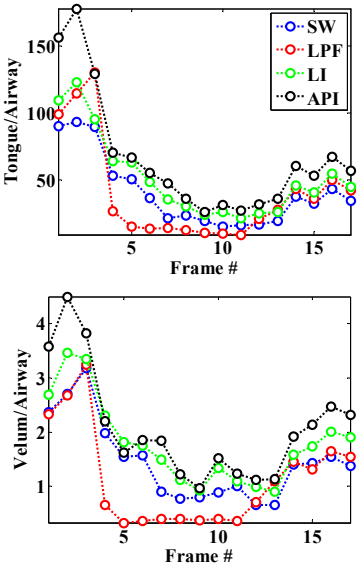

Fig. 3: Average energy in the tongue (top) and velum (bottom) regions, normalized by the airway energy. Larger values indicate higher discriminability of anatomy boundaries.

References:

[1] Liang, et al. Intl. J. Imaging Syst. Technol. 1997;8: 551-557.
[2] Tao, et al. MRM 2003;50:1031-1042.